J. Non-Equilib. Thermodyn.
2005 · Vol. 30 · pp. 151–162

Transport of O_2 from arterioles

Silvia Bertuglia[1], Alfonso Limon[2], Bjarne Andresen[2,3,*], Karl Heinz Hoffmann[4], Christopher Essex[3,5] and Peter Salamon[2]
[1] CNR, Institute of Clinical Physiology, University of Pisa, I-56100 Pisa, Italy
[2] Department of Mathematical Sciences, San Diego State University, San Diego, CA 92182-7720, USA
[3] Ørsted Laboratory, University of Copenhagen, Universitetsparken 5, DK-2100 Copenhagen Ø, Denmark
[4] Institute of Physics, Chemnitz University of Technology, D-09107 Chemnitz, Germany
[5] Department of Applied Mathematics, University of Western Ontario, London, Ontario N6A5B7, Canada

*Corresponding author (andresen@fys.ku.dk)

Abstract

Oxygen delivery to the tissues is crucial to survival but our understanding of the processes involved in the transport of oxygen from blood to tissue is incomplete. The aim of the present work is to illustrate a long-standing paradox regarding such transport by reporting new state-of-the-art measurements and by analyzing the results in several ways, thereby exploring possible resolutions of the paradox. Our model calculations show that slight extensions of system parameters are sufficient to overcome the apparent inconsistencies. Alternatively, so far unappreciated mild effects like flow-assisted diffusion in the interstitium will explain the supernormal diffusion of oxygen.

1. Introduction

Historically, the Krogh diffusion model has been accepted as the proper way to describe the delivery of O_2 from the blood stream to the interstitium [1]. While Krogh intended this description to relate entirely to capillaries, several workers [2–5] later showed that most of the transport in fact comes from arterioles. This conclusion is based on measurements of changes in O_2 content of the blood within the arterioles.

These measurements however have not been reconciled with possible mechanisms of O_2 transport away from the arterioles. In fact, the present understanding of the transport of O_2 from the blood stream to the interstitium is fraught with controversy. Unfortunately, the available experimental data are insufficient to make a clear decision. In this paper, we report new state-of-the-art measurements of O_2 concentrations

 DOI 10.1515/JNETDY.2005.011

in and around arterioles, review the facts surrounding this controversy, and suggest some possible mechanisms for O_2 transport that might explain the discrepancies. On the one hand, model calculations show that simple diffusive transport is not in contradiction to the experimental data if system parameters are allowed to take on values at the limits of their uncertainty intervals. On the other hand, additional mild effects like flow-assisted diffusion in the interstitium arising from known arteriolar pulsation are argued to be able to easily overcome the discrepancies.

2. Experiment

An automated system based on phosphorescence quenching was used to measure oxygen tension p_{O2} within the microcirculation of the hamster cheek pouch. We measured the intraluminal and perivascular distribution of oxygen gradients in the arterioles, venules, and interstitium of the microcirculation visualized by transmitted light.

Measurements of p_{O2} demonstrated that there was a progressive fall in oxygen tension from the largest arterioles entering a tissue down to the terminal arterioles in hamster cheek pouch microcirculation [6]. These measurements are based on the relationship between the rate of decay of excited palladium-mesotetra-(4-carboxyphenyl) porphyrin bound to albumin and the local p_{O2} value. The albumin-bound probe enables measurement of oxygen levels in the blood as well as in the tissue since the probe passes into the interstitium according to the exchange of albumin from blood to tissue. The hamster cheek pouch, an epithelial tissue, has been used extensively to study microcirculation [7–10].

2.1. Materials and methods

A group of 25 male Syrian hamsters (80–100 g; Charles River, Italy) were anesthetized by intraperitoneal injections of sodium pentobarbital, 50 mg/kg body wt. The animals were tracheotomized and the right carotid artery and femoral vein were cannulated to measure blood pressure and to inject the phosphorescence probe and supplementary doses of anesthetic. The cheek pouch was surgically prepared as previously reported [5]. It was spread over a plexiglas microscope stage and a region of about 1 cm^2 in area was prepared as a single layer for intravital microscopic observations. The cheek pouch was then covered with transparent plastic film to prevent both desiccation of the tissue and gas exchange with the atmosphere. Observations were made with an intravital microscope (Orthoplan; Leica Microsystem GmbH, Wetzlar, Germany) using the trans-illumination technique. The p_{O2} measurements were performed at several locations in the microcirculation. All selected microvessels and interstitial tissue segments were also recorded by a video camera (Cohu Inc., San Diego CA, USA), displayed on a monitor, and transferred to a video recorder. The hamster's body temperature and cheek pouch temperature were maintained at 37°C with circulating warm water. At the conclusion of the experiment, an intravenous injection of pentobarbital (300 mg/kg bw) was used as the method of euthanasia. Animal handling and care were provided following the procedures outlined in the

"Guide for the Care and Use of Animals in the Laboratories of the Italian Research Council".

2.2. The p_{O2} measurement system

The oxygen-dependent quenching of the phosphorescence decay method is based on light emitted by albumin-bound palladium-mesotetra-(4-carboxyphenyl) porphyrin [11]. Pd-porphyrin is excited to its triplet state by exposure to pulsed light, after which phosphorescence intensity is reduced by emission and energy transfer to O_2. The relationship between phosphorescence lifetime and oxygen tension is given by the Stern-Volmer equation,

$$1/\tau = 1/\tau_0 + k_q p_{O2}, \tag{1}$$

where τ_0 and τ are the phosphorescence lifetimes in the absence of molecular oxygen and at a given p_{O2}, respectively, and k_q is the quenching constant. Both factors are pH and temperature dependent.

Palladium-mesotetra-(4-carboxyphenyl) porphyrin (Porphyrin Products, Logan, UT, USA) bound to serum albumin and diluted in saline (0.9% sodium chloride, Elkins-Sinn) to a final concentration of 15 mg/ml was used as a phosphorescent dye ($\tau_0 = 600$ μs, $k_q = 325$ Torr^{-1} s^{-1} at pH 7.4 and 37°C) and intravenously injected (15 mg/kg bw). Phosphorescence was excited by light pulses (30 Hz) generated by a 45 W xenon strobe arc (EG&G Electro Optics, Salem, MA, USA). The pulsed light illuminated a round area of ~140 μm diameter, while p_{O2} measuring sites were microscopically selected by an adjustable slit. The slit size was fixed at 5–15 μm × 20 μm for microvascular measurements and positioned longitudinally over the center of the blood vessels so that only the main blood stream was covered and any overlapping with the vessel wall was strictly avoided (see Figure 1). For interstitial tissue p_{O2} measurements, the slit was positioned on intercapillary segments, avoiding any spatial interference with underlying or adjacent blood vessels. Filters of 420 and 630 nm were used for porphyrin excitation and phosphorescence emission, respectively. Phosphorescence signals were captured by a photomultiplier (EMI, 9855B; Knott Elektronik, Munich, Germany).

The decay curves were averaged, visualized, and saved by a digital oscilloscope (Hitachi Oscilloscope V-1065, 100 MHz; Hitachi, Denshi, Japan). Decay time constants were determined by a computer fitting the averaged decay curves to a single exponential using the Stern-Volmer equation (1). The microvascular measurements were initiated 2 min after injection of the dye, while interstitial tissue p_{O2} was measured after a period of 15 min, allowing enough porphyrin to permeate the tissue for sufficient extravascular phosphorescence signal strength.

Systemic parameters recorded consisted of arterial blood gases, mean arterial pressure, and hematocrit. The mean arterial pressure (Viggo-Spectramed P10E2 transducer, Oxnard, CA, USA, connected to a catheter in the carotid artery) and heart rate were monitored by a Gould Windograf recorder (Mod. 13-6615-10S; Gould

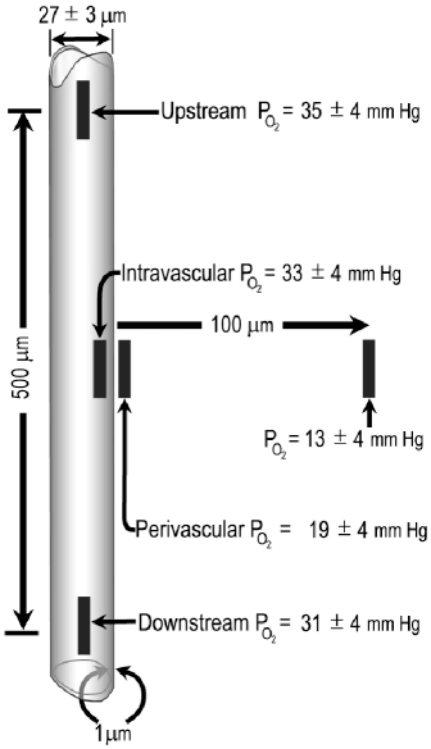

Figure 1 Schematic picture of the geometric setup for the experiment and the model. Values shown are the results of the experiment.

Inc., Ohio, IL, USA). Data were recorded and stored in a computer. Quantitative data are given as mean values ± standard deviations. Comparisons of dependent variables over the observation period were tested using the paired Student's *t*-test and Bonferroni probabilities for repeated measurements. Results with error probability less than 0.05 were considered significant.

3. Results

For the purpose of comparison to the model calculations below, we restrict the discussion of the experimental results to our findings for A2 arterioles. The measurements obtained are summarized in Figure 1. For the rest of the experimental results, see [5].

3.1. Oxygen depletion from arteriolar blood

As shown in Figure 1, the oxygen tension is measured to drop from $p_{O2} = 35$ to 31 mm Hg over a distance of $l = 500$ μm along the arteriole, inducing a drop from

$S = 42$ to 35%, i.e., $\Delta S = 7\%$, in hemoglobin (Hb) saturation according to standard Hb calibration curves (see, e.g., [12]). The carrying capacity of hemoglobin at 100% saturation is $k = 0.061$ mol O_2/kg (1.36 ml O_2 per g of hemoglobin), and the hemoglobin content of whole blood in hamsters is $H = 650$ kg/m^3 at the normal hematocrit of $h_{\text{artery}} = 44$. Since the hematocrit in arterioles is only $h_{\text{arteriole}} = 18$, this drop of $\Delta S = 7\%$ saturation corresponds to a depletion of the oxygen concentration of

$$\begin{aligned}\Delta C_{\text{blood}} &= \Delta S \times k \times H \times h_{\text{arteriole}}/h_{\text{artery}} \\ &= 7\% \times 0.061 \text{ mol } O_2/\text{kg} \times 650 \text{ kg/m}^3 \times 18/44 \\ &= 1.1 \text{ mol } O_2/\text{m}^3 \text{ blood} \end{aligned} \tag{2}$$

over the 500-μm-long segment of arteriole. A measured linear blood flow velocity of $v = 2.0$ mm/s through a vessel of diameter $d = 27$ μm gives a volumetric flow of

$$V = \pi/4 \times d^2 \times v = \pi/4 \times (2.7 \times 10^{-5} \text{ m})^2 \times 0.0020 \text{ m/s} = 1.1 \times 10^{-12} \text{ m}^3/\text{s}. \tag{3}$$

Combining Eqs. (2) and (3) we finally arrive at an oxygen depletion rate of

$$F_{\text{depl}} = \Delta C_{\text{blood}} \times V = 1.3 \times 10^{-12} \text{ mol } O_2/\text{s} \tag{4}$$

over l, or at standard temperature and pressure 2.7×10^{-8} ml O_2/s. Per surface area $A = \pi dl$ of the vessel, this amounts to

$$f_{\text{depl}} = F_{\text{depl}}/A = 3.0 \times 10^{-5} \text{ mol/m}^2\text{s} = 6.7 \times 10^{-13} \text{ ml } O_2/(\mu\text{m})^2\text{s}, \tag{5}$$

in agreement with related observations [13, Table 4].

3.2. Diffusive transport out of the arteriole

Again referring to Figure 1, the oxygen tension drops from $p_{O2} = 33$ to 19 mm Hg across the vessel wall, i.e., $\Delta p_{\text{wall}} = 14$ mm Hg. This oxygen pressure difference only concerns oxygen physically dissolved in the plasma and interstitial fluid, where at a partial pressure of 100 mm Hg the solubility is $\sigma_{100} = 0.13$ mol/m^3 = 0.3 ml of O_2 per 100 ml of plasma (see, e.g., [12]). Thus this change in tension corresponds to a difference in oxygen concentration of

$$\begin{aligned}\Delta C_{\text{plasma}} &= \Delta p_{\text{wall}} \times \sigma_{100} \\ &= (14 \text{ mm Hg}/100 \text{ mm Hg}) \times 0.13 \text{ mol/m}^3 \\ &= 0.019 \text{ mol } O_2/\text{m}^3. \end{aligned} \tag{6}$$

If oxygen is transported through the arteriolar wall exclusively by simple diffusion and we take the wall thickness to be $w = 1$ μm corresponding to a single layer of endothelial cells, this amounts to a diffusive flow per surface area of the vessel of

$$f_{\text{diff}} = D \times \Delta C_{\text{plasma}}/w$$
$$= 2 \times 10^{-9}\ \text{m}^2/\text{s} \times 0.019\ \text{mol/m}^3/1\ \mu\text{m} = 3.7 \times 10^{-5}\ \text{mol/m}^2\text{s}$$
$$= 8.5 \times 10^{-13}\ \text{ml O}_2/(\mu\text{m})^2\text{s} \quad (7)$$

using a typical diffusion constant in tissue of $D = 2 \times 10^{-9}$ m^2/s $= 2 \times 10^{-5}$ cm^2/s (see, e.g., [12]).

Within the accuracy of the measurements, this flow is the same as the depletion flow, Eq. (5). Thus, under the specified assumptions, simple diffusion is fully capable of accounting for oxygen transport from arterioles to the tissue immediately surrounding them. If, on the other hand, we consider an arteriole surrounded by a single layer of muscle fibers yielding a typical wall thickness of $w = 6$ μm [13], the gradient and consequently the diffusion rate would be reduced by a factor 6 to $f_{\text{diff}} = 1.4 \times 10^{-13}$ ml O$_2$/(μm)^{2}s surface area of the vessel. In spite of the relatively large uncertainties of the measurements, this value is distinctly smaller than f_{depl}, Eq. (5), and probably implies additional effects. The model calculations below will elucidate the respective possibilities.

3.3. Diffusive transport through tissue

Using the same arguments as in the previous subsection on the oxygen tension data in the tissue (see Figure 1), we now find a drop in oxygen tension from $p_{\text{O2}} = 19$ to 13 mm Hg across $x = 100$ μm of tissue, i.e., $\Delta p_{\text{tissue}} = 6$ mm Hg. This leads to a typical concentration gradient of 85 mol/m^4. Using again the diffusion constant in tissue of $D = 2 \times 10^{-9}$ m^2/s $= 2 \times 10^{-5}$ cm^2/s, we arrive in an order of magnitude estimate at a flow per surface area of the vessel of only

$$f_{\text{tissue}} = D \times \Delta C_{\text{tissue}}/x$$
$$= 1.7 \times 10^{-7}\ \text{mol/m}^2\text{s} = 3.6 \times 10^{-15}\ \text{ml O}_2/(\mu\text{m})^2\text{s}, \quad (8)$$

which is one to two orders of magnitude smaller than the depletion flow f_{depl} leaving the blood stream, Eq. (5).

4. The paradox

The oxygen flux out of arterioles as measured and calculated above is in good agreement with many previously reported values (see [13, Table 4]). The difficulty begins when one tries to account for the distribution of this oxygen. While the measured gradient across the arteriolar wall is likely sufficiently large to allow this much O_2 to diffuse out of the arteriole (see above), the O_2 gradient through the interstitium appears to be too small by at least one order of magnitude to carry this O_2 to any significant distance from the wall. To resolve this paradox, a number of hypotheses have been advanced by leading workers in microcirculation, including the possibility that: (i) over 90% of the O_2 is consumed in the arteriolar wall [4]; (ii) several independently measured O_2 depletion values are incorrect by one to two orders of magnitude [13];

or (iii) the effective diffusion coefficient of O_2 through tissue is an order of magnitude larger than normal diffusion [6]. Such supernormal diffusion could be caused by pulsating action of the muscle fibers around the arterioles or by flow-assisted diffusion within the tissue cells. As an aid to discussing these and other possibilities, we introduce the model presented in the following section.

5. Model

The model we analyze consists of three concentric cylinders [13]. The inner cylinder with radius r_i is the lumen of the arteriole. The second cylinder has radius r_o and extends from r_i to the outside of the arteriolar wall; i.e., it is the wall. The outer third cylinder has radius r_t and includes the region of interstitium supplied by the arteriole, i.e., from r_o and outward. We assume full cylindrical symmetry and thus there is no angular dependence of the variables. In addition, we assume translational symmetry along the z-axis; i.e., we consider a two-dimensional model. Note that this assumes that flows and concentrations do not change along the length of the arteriole. Finally, we assume steady-state conditions, thereby eliminating any time dependence.

With these assumptions, the diffusion equation in cylindrical coordinates reduces to a one-dimensional differential equation. Let S_w be the rate at which oxygen is consumed in the wall per unit volume and D_w be the diffusion constant for oxygen within the wall. The oxygen concentration $p(r)$ inside the wall then must satisfy

$$\frac{1}{r}\frac{d}{dr}\left(r\frac{dp}{dr}\right) = \frac{d^2p}{dr^2} + \frac{1}{r}\frac{dp}{dr} = \frac{S_w}{D_w}. \tag{9}$$

Solving this differential equation with the boundary conditions $p(r_i) = p_i$ and $p(r_o) = p_o$ leads to

$$p(r) = p_i + \frac{S_w(r^2 - r_i^2)}{4D_w} + \left(p_i - p_o + \frac{S_w(r_o^2 - r_i^2)}{4D_w}\right)\frac{\ln(r/r_i)}{\ln(r_i/r_o)}, \tag{10}$$

from which oxygen flows can be determined through the concentration gradients using

$$J = -D_w\frac{dp}{dr}. \tag{11}$$

Introducing variables J_i and J_o for the values of the flow at r_i and r_o, we solve for D_w and S_w getting

$$D_w = \frac{2(J_i r_i - J_o r_o)}{p_o - p_i} + \frac{r_o r_i (J_o r_i - J_i r_o)}{(p_o - p_i)(r_o^2 - r_i^2)}\ln\left(\frac{r_o}{r_i}\right), \tag{12}$$

$$S_w = \frac{2(J_o r_o - J_i r_i)}{(r_i^2 - r_o^2)}. \tag{13}$$

We next repeat this calculation for the region between r_o and r_t getting

$$D_t = \frac{2(J_o r_o - J_t r_t)}{p_t - p_o} + \frac{r_t r_o (J_t r_o - J_o r_t)}{(p_t - p_o)(r_t^2 - r_o^2)} \ln\left(\frac{r_t}{r_o}\right), \tag{14}$$

$$S_t = \frac{2(J_t r_t - J_o r_o)}{(r_o^2 - r_t^2)}, \tag{15}$$

where D_t and S_t are the diffusion constant and consumption rate for O_2 in the tissue.

The above calculations express the consumption rates and the diffusion constants in terms of the concentrations and the fluxes at the respective radii. The values of the concentrations $p_i = 33$ mm of Hg, $p_o = 19$ mm of Hg, and $p_t = 13$ mm of Hg and the flow $J_i = 3.0 \times 10^{-17}$ mol/(μm)^{2}s are taken from the experiment Eq. (5), while $J_t = 0$ is based on the assumption that p_t is the minimum pressure present.

This leaves us with four equations (12–15) for determining the five parameters D_w, D_t, J_o, S_w, S_t. To explore possible resolutions of the aforementioned paradox, we use the equations to plot consistent values of our parameters. We also explore possible effects of uncertainty in geometrical factors such as the thickness of the arteriolar wall, $r_o - r_i$, and the thickness of the region supplied by the arteriole, $r_t - r_o$. The plots in Figure 2 show the ratio of the diffusion constants in the tissue and the arteriolar wall, D_t/D_w, as a function of r_t/r_i for wall thickness $r_o - r_i$ equal to 1 μm (Figure 2a), 3 μm (Figure 2b), 6 μm (Figure 2c), and 9 μm (Figure 2d). The three curves in each figure correspond to S_w/S_t values of 0, 1, and 10, respectively; i.e., no oxygen consumption in the wall, the same rate, and 10 times the consumption rate in tissue. Figure 3a–d presents a different view of the same information, this time plotting S_w/S_t as a function of r_t/r_i for the various wall thicknesses with the different curves corresponding to D_t/D_w values of 1, 2, and 5, respectively.

6. Discussion

The results from our model calculations provide a framework for considering possible resolutions of the paradox. Recall that the paradox results from using our measured geometric values in Figure 1 along with the traditional view that O_2 moves freely through all tissues ($D_t/D_w \approx 1$) while most of the O_2 delivered is used in the tissues (and thus, considering the volumes of the respective regions, $S_w/S_t <\approx 10$).

In our calculations, we have included a multitude of geometrical scenarios besides the measured values shown in Figure 1. Our reason for considering different wall thicknesses is that portions of the arterioles are likely to be surrounded by a layer of smooth muscle. In the calculations by Vadapalli et al. [13], they use a value of 6.5 μm for the wall thickness of comparable size arterioles. In addition, we wanted to account for the uncertainty in the position where the concentration p_o applies.

Our reason for considering a large range of possible r_t values is to account for uncertainty in the size of the region supplied by the arteriole. Since true three-dimensional

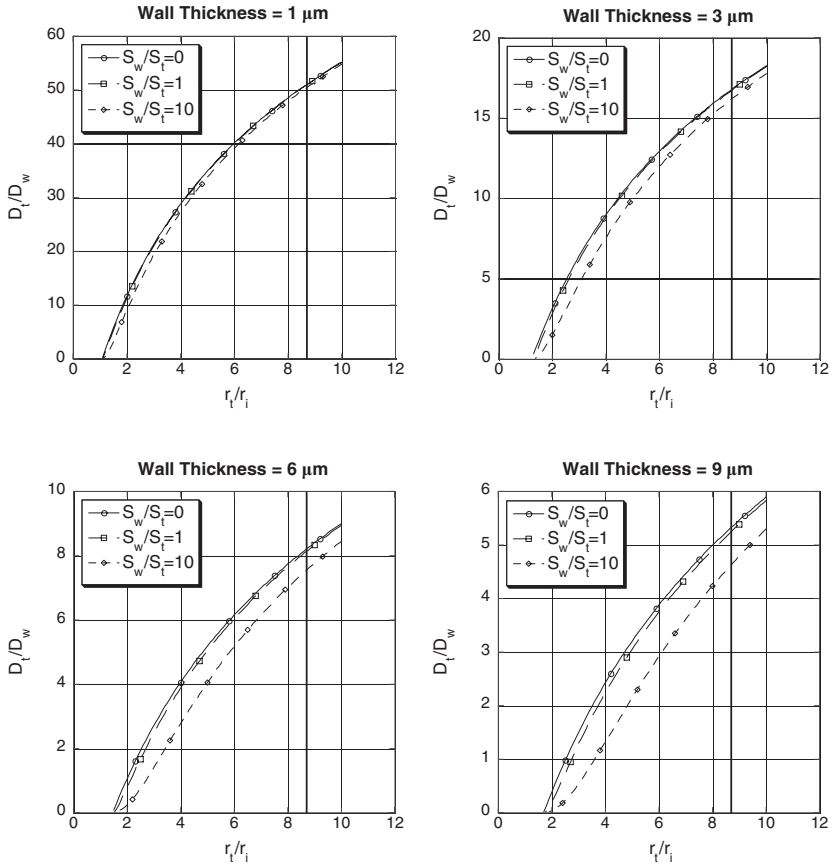

Figure 2 Diffusion enhancement factors as a function of the linear size of the interstitial basin supplied by the arteriole for various wall thicknesses and the ratio of consumption rates in the wall and in the interstitium. The vertical lines indicate the values as measured in the experiment.

resolution of the local microvasculature is not available, it is not possible to assert with any confidence that other blood vessels, e.g. capillaries, did not in fact supply O_2 to the apparent point of minimum O_2 concentration 100 μm from the arteriole. Future investigations could eliminate this uncertainty by using recently developed femtosecond laser technology [14] to completely map the local three-dimensional structure of the microvasculature examined.

The hypothesis advanced by Vadapalli et al. [13] is that the p_{O2} measurements made by several independent groups share a systematic error of one to two orders of magnitude for the deduced O_2 depletion. They were led to this conclusion because 15 years of efforts since [6] have not led to any resolution. We nonetheless find the conjecture that several workers (including us) have been measuring O_2 disappearance incorrectly to be untenable.

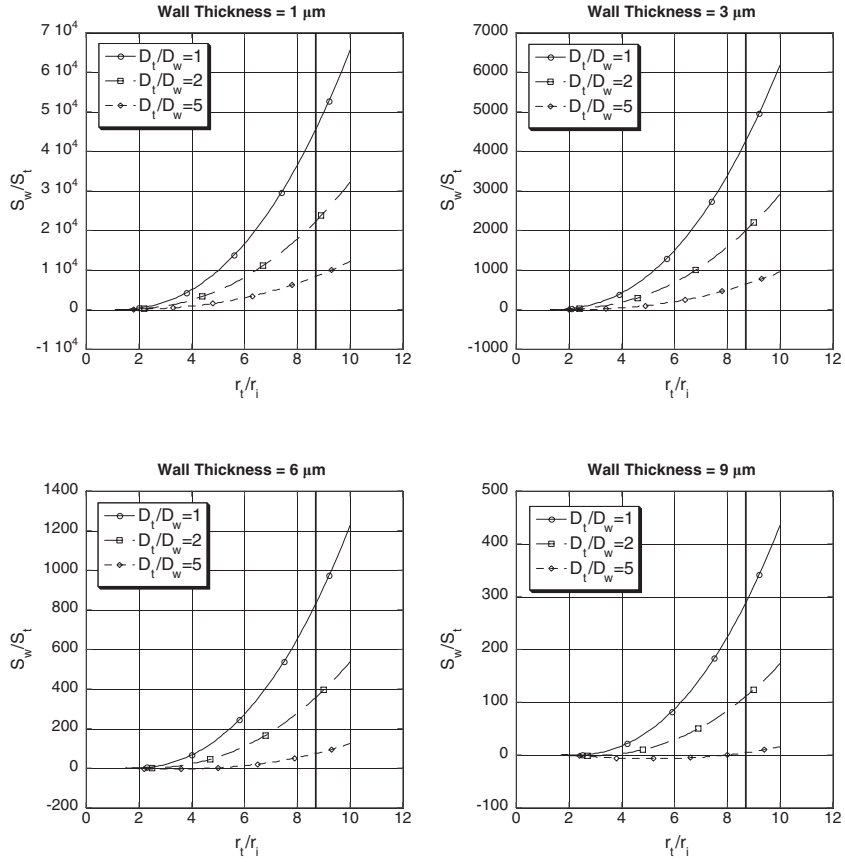

Figure 3 The ratio of consumption rates in the wall and in the interstitium as a function of the linear size of the interstitial basin supplied by the arteriole for various wall thicknesses and diffusion enhancement factors. The vertical lines indicate the values as measured in the experiment. Note that for a wall thickness of 9 μm and a diffusion enhancement of 5, the resulting consumption ratios fall outside the physical range and take on negative values.

We now turn to consider possible resolutions of the paradox. Intaglietta's proposed resolution [4, 15] is to assume that most of the O_2 flux does not actually make it into the interstitium, being consumed in the vessel wall. Vadapalli et al. [13] do a very careful job disproving this hypothesis by calculating an upper bound to the amount of O_2 that could possibly be consumed in the wall and find a value well below what would be required to account for enough O_2 disappearance. We find Intaglietta's hypothesis untenable also on the general grounds that it would require most of the metabolic benefits of distributing O_2 to the tissues to be spent just on achieving the distribution.

Most credible among the resolutions heretofore suggested is the original hypothesis by Popel et al. [6], which claimed that O_2 transport through the tissue is faster than

normal by an order of magnitude. While our analysis suggests compromise solutions that require less than a full order of magnitude increase in extravascular diffusion, some enhancement of the effective diffusion rate is clearly required. Diffusion rates are known to be enhanced by one to two orders of magnitude by even a slight amount of convective flow, especially if any mixing is present. Some convective flow is created by the pulsatile vasomotor change of arterioles [16]. Purely periodic flows in themselves transport nothing of course. Fluid elements simply move out and come back to where they started with no net transport of anything. However, if this motion is in conjunction with dissipative mechanisms such as the pervasive physiological diffusion or other chemical fractionation or mixing processes, the interacting fluid elements piggybacked on the flow interact with more tissue than otherwise, thus considerably accelerating transport.

Another mechanism for enhancing the diffusion comes from the fact that much of the transport occurs through cells that have internal mechanisms such as cytoplasmic streaming for mixing their fluid contents. Another argument for the need for enhanced diffusion through tissue comes from the fact that under extreme load the oxygen turnover in a muscle cell may increase 80-fold over the resting state [17]. Assuming purely diffusive transport, this would require a corresponding 80-fold increase in the gradient of the oxygen tension.

On the basis of the above framework, we see that provided we are willing to accept a modest enhancement in diffusion rates through tissue, there is a range of parameter values that make the paradox disappear. For instance, the combination of higher burning rates in the vessel wall, $S_w/S_t \approx 10$, enhanced diffusion, $D_t/D_w \approx 3$, restricted basin to be supplied by the arteriole, $r_t/r_i \approx 4$, and a wall thickness of 6 μm (see Figure 2c) account for the measured disappearance of O_2. Even for equal burning rates, $S_w/S_t \approx 1$, a 4-fold enhancement of the effective diffusion rate in tissue, $D_t/D_w \approx 4$, suffices.

Considering the fairly large uncertainties in the experimental data (see Figure 1), any model will allow a fair variation of its parameters as suggested above. By the same token, more elaborate models than the one considered here cannot be justified. Finally, it should be mentioned that the reaction–diffusion problem in chemical engineering is related to the present model.

7. Conclusions

In the present paper, we have described a long-standing paradox concerning the delivery of oxygen to the tissues through the microvasculature. We presented experimental results that illustrate the paradox and performed calculations on a model that provides a framework for possible resolutions. The calculations show that the discrepancies can be made to disappear if the various physical effects involved are all allowed to pull in the same direction. A different resolution is obtained if one considers the possible consequences of known phenomena like arteriolar pulsation, which may power flow-assisted diffusion in the interstitium. Such effects can greatly increase the apparent diffusion rate of oxygen.

Acknowledgements

This work was supported in part by the Danish Natural Science Research Council, contract 21-01-0352. The authors thank San Diego State University and CNR Institute of Clinical Physiology, Pisa, Italy for their hospitality. Much of the present work was the result of discussions in the fertile atmosphere of the Telluride Summer Research Center.

References

[1] Krogh, A., The number and distribution of capillaries in muscle with the calculation of the oxygen pressure necessary for supplying the tissue, J. Physiol., 52 (1918), 409–515.
[2] Duling, B.R., Microvascular responses to alterations in oxygen tension, Circ. Res., 31 (1972), 481–489.
[3] Ellsworth, M.L., Pittman, R.N., Arterioles supply oxygen to capillaries by diffusion as well as by convection, Am. J. Physiol. Heart Circ. Physiol., 258 (1990), H1240–H1243.
[4] Intaglietta, M., Johnson, P.C., Winslow, R.M., Microvascular and tissue oxygen distribution. A review, Cardiovasc. Res., 32 (1996), 632–643.
[5] Bertuglia, S., Giusti, A., Microvascular oxygenation, oxidative stress, NO suppression and superoxide dismutase during postischemic reperfusion, Am. J. Physiol. Heart Circ. Physiol., 285 (2003), H1064–H1071.
[6] Popel, A.S., Pittman, R.N., Ellsworth, M.L., The rate of oxygen loss from arterioles is an order of magnitude higher than expected, Am. J. Physiol. Heart Circ. Physiol., 256 (1989), H921–H924.
[7] Pawlowski, M., Wilson, D.F., Monitoring of the oxygen pressure in the blood of live animals using the oxygen dependent quenching of phosphorescence, Adv. Exp. Med. Biol., 316 (1992), 179–185.
[8] Duling, B.R., Berne, R.M., Longitudinal gradients in periarteriolar oxygen tension in hamster cheek pouch, Fed. Proc., 29 (1970), A320.
[9] Segal, S.S., Duling, B.R., Flow-control among microvessels coordinated by intercellular conduction, Science, 234 (1986), 868–870.
[10] Bartlett, I.S., Segal, S.S., Resolution of smooth muscle and endothelial pathways for conduction along hamster cheek pouch arterioles, Am. J. Physiol. Heart Circ. Physiol., 278 (2000), H604–H612.
[11] Kerger, H., Torres Filho, I.P., Rivas, M., Winslow, R.M., Intaglietta, M., Systemic and subcutaneous microvascular oxygen tension in conscious Syrian golden hamsters, Am. J. Physiol. Heart Circ. Physiol., 267 (1995), H802–H810.
[12] Alberts, B., Johnson, A., Lewis, J., Raff, M., Roberts, K., Walter, P., Molecular Biology of the Cell, Garland Science, New York, 2002.
[13] Vadapalli, A., Pittman, R.N., Popel, A.S., Estimating oxygen transport resistance of the microvascular wall, Am. J. Physiol. Heart Circ. Physiol., 279 (2000), H657–H671.
[14] Tsai, P.S., Friedman, B., Ifarraguerri, A.I., Thompson, B.D., Lev-Ram, V., Schaffer, C.B., Xiong, Q., Tsien, R.Y., Squier, J.A., Kleinfeld, D., All-optical histology using ultrashort laser pulses, Neuron, 39 (2003), 27–41.
[15] Tsai, A.G., Friesenecker, B., Mazzoni, M.C., Kerger, H., Buerk, D.G., Johnson, P.C., Intaglietta, M., Microvascular and tissue oxygen gradients in the rat mesentery, Proc. Natl. Acad. Sci. USA, 95 (1998), 6590–6595.
[16] Bertuglia, S., Colantuoni, A., Coppini, G., Intaglietta, M., Hypoxia- or hyperoxia-induced changes in arteriolar vasomotion in skeletal muscle microcirculation, Am. J. Physiol. Heart Circ. Physiol., 260 (1991), H362–H372.
[17] Hochachka, P.W., The metabolic implications of intracellular circulation, Proc. Natl. Acad. Sci. USA, 96 (1999), 12233–12239.

Paper received: 2004-10-12
Paper accepted: 2004-12-14